New Insights Into the Substorm Initiation Sequence From the Spatio-Temporal Development of Auroral Electrojets

S. Ohtani[1] , **T. Motoba[1]** , **J. W. Gjerloev[1]** , **H. U. Frey[2]** , **I. R. Mann[3]** , **P. J. Chi[4]** , and **H. Korth[1]**

[1]Johns Hopkins University Applied Physics Laboratory, Laurel, MD, USA, [2]Space Sciences Laboratory, University of California, Berkeley, CA, USA, [3]University of Alberta, Edmonton, CA, USA, [4]Department of Earth and Space Sciences, University of California, Los Angeles, CA, USA

Abstract In the present study we examine three substorm events, Events 1–3, focusing on the spatio-temporal development of auroral electrojets (AEJs) before auroral breakup. In Events 1 and 2, auroral breakup was preceded by the equatorward motion of an auroral form, and the ground magnetic field changed northward and southward in the west and east of the expected equatorward flow, respectively. Provided that these magnetic disturbances were caused by local ionospheric Hall currents, this feature suggests that the equatorward flow turned both eastward and westward as it reached the equatorward part of the auroral oval. The auroral breakup took place at the eastward-turning and westward-turning branches in Events 1 and 2, respectively, and after the auroral breakup, the westward AEJ enhanced only on the same side of the flow demarcation meridian. The zonal flow divergence is considered as an ionospheric manifestation of the braking of an earthward flow burst in the near-Earth plasma sheet and subsequent dawnward and duskward turning. Therefore, in Events 1 and 2, the auroral breakup presumably mapped to the dawnward and duskward flow branches, respectively. Moreover, for Event 3, we do not find any pre-onset auroral or magnetic features that can be associated with an equatorward flow. These findings suggest that the braking of a pre-onset earthward flow burst itself is not the direct cause of substorm onset, and therefore, the wedge current system that forms at substorm onset is distinct from the one that is considered to form as a consequence of the flow braking.

1. Introduction

Substorm initiation is often addressed in terms of the formation of the substorm current wedge by the braking of earthward flow bursts in the near-Earth magnetosphere (e.g., Birn et al., 1999; Yang et al., 2012); see also a review by Kepko et al. (2015). Such flow bursts are widely considered as the interchange motion of depleted magnetic flux tubes, which form as an earthward ejecta of magnetotail reconnection (Wolf et al., 2009). In fact, previous studies reported the pre-onset occurrence of tailward flows with southward magnetic fields in the plasma sheet (e.g., Machida et al., 1999; Nagai et al., 1998; Ohtani et al., 1999), which is widely accepted as a manifestation of tail reconnection and a counterpart of earthward flow bursts.

This sequence of substorm initiation is often referred to as the outside-in model (e.g., Shiokawa et al., 1997). The idea is that magnetic reconnection in the mid-tail precedes a near-Earth process, which the model does not specify but considers as an essential element of substorm initiation. The onset of auroral substorms (Akasofu, 1964), which takes place several degrees equatorward of the open-closed boundary (e.g., Friedrich et al., 2001; Samson et al., 1992), is generally considered as an auroral manifestation of this near-Earth process, and it has been discussed from various aspects such as the formation of substorm current wedge (e.g., McPherron et al., 1973) and tail current disruption as a consequence of a local plasma instability (e.g., Lui, 1996). Here one issue that is essential for understanding substorm initiation in terms of the outside-in model but is rarely addressed explicitly is whether the braking of earthward flow bursts creates a favorable condition for the near-Earth onset process (as originally proposed by the outside-in model), or the flow braking itself is the direct cause of substorm onset.

The causal link between earthward flow bursts and substorm initiation is also suggested by auroral observations (e.g., Kepko et al., 2009; Lyons et al., 2010; Nishimura et al., 2010a). It is widely accepted that equatorward moving auroral forms, especially auroral streamers, are an auroral manifestation of earthward flow bursts in the plasma sheet (Henderson et al., 1998; Juusola et al., 2009; Kauristie et al., 2000; Nakamura et al., 2001; Sergeev et al., 1999; Zesta et al., 2000). Therefore, the observation that auroral breakup is traced back to an auroral streamer, whether directly or through either eastward and westward turning (Nishimura et al., 2010a), seems
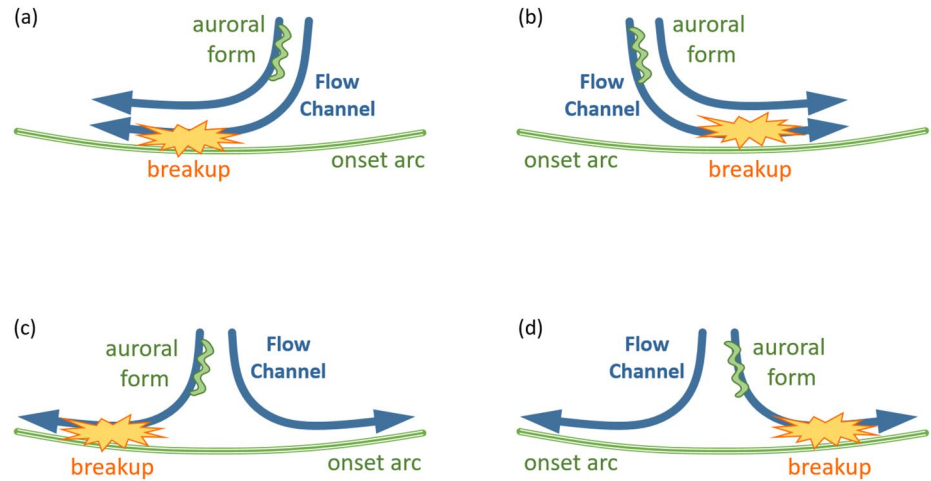
Figure 1. Schematic illustration of the location of auroral breakup relative to the pre-onset equatorward flow channel. The flow channel (a) turns westward, (b) turns eastward, (c) diverges followed by auroral breakup at the westward branch, and (d) diverges followed by auroral breakup at the eastward branch. The accompanying equatorward-moving auroral form may or may not be an auroral streamer, and the onset arc may pre-exist or may form after the approach of the equatorward flow.

to support the idea that substorms are triggered by the penetration of earthward flow bursts into the near-Earth region. It is also noteworthy that preceding auroral streamers often appear to follow stream lines of ionospheric convection in the Harang reversal (Nishimura et al., 2010a), which is consistent with the well-known tendency that auroral breakup very often takes place at premidnight (e.g., Frey et al., 2004; Gjerloev et al., 2007; Liou et al., 2001).

Figure 1 schematically shows four different scenarios regarding the evolution of an equatorward flow and the location of subsequent auroral breakup. For the sake of discussion, we consider that the auroral breakup takes place either east or west of the flow channel even though auroral breakup often occurs where the equatorward front reaches the equatorward part of the auroral oval (Nishimura et al., 2010a). First, let us assume that the auroral breakup takes place after the auroral streamer turns westward. The associated equatorward flow may also turn westward as shown in Figure 1a, or may diverge eastward and westward but with the auroral streamer following only the westward turning branch as shown in Figure 1c. The two cases are difficult to distinguish with auroral images alone especially for events in the Harang sector. For the eastward turning, we can consider a similar pair of possibilities as shown in Figures 1b and 1d. In Figures 1a and 1b the ionospheric footprint of the flow braking can be anywhere along the flow channel before the onset location. For Figures 1c and 1d, in contrast, the braking point presumably maps to where the equatorward flow diverges eastward and westward, and it is not obvious, especially for Figure 1d, how, or if, the auroral breakup can be explained if the formation of the substorm current wedge is a direct consequence of the flow braking. Note that the wedge current system generated by the flow braking should be centered at the flow demarcation meridian, and therefore, its upward field-aligned current (FAC), which is presumably accompanied by auroral intensification, is considered to be distributed mostly west of this meridian. Thus, understanding how the equatorward flow behaves prior to auroral breakup must be a critical step to understanding the role of the flow braking in the substorm initiation.

It may be debatable how often auroral breakup follows the reported auroral sequence, whether they are full substorm onsets, pseudobreakups, or intensifications (Frey, 2010; Mende et al., 2011; Murphy et al., 2014; Nishimura et al., 2010b). Nevertheless, the reported sequence is observed repeatedly, if not for every substorm, and therefore, it should provide an important insight into the substorm initiation process. In the present study we seek to identify where the flow braking takes place in the auroral sequence, and address its role in substorm initiation.

For this purpose we need to address longitudinal ionospheric convection over several hours in magnetic local time (MLT) at a sub-minute time resolution; substorm onset usually takes place within a few minutes after the preceding auroral streamer reaching the equatorward portion of the auroral oval (Nishimura et al., 2010a). Those requirements are rather difficult to meet with currently available radar measurements, although it is preferable to examine direct observations of ionospheric convection flows. In the present study we infer the pre-onset

Table 1
Geographic Longitude and Latitude (GLon and GLat), and Geomagnetic Longitude and Latitude (MLon and MLat) of Ground Stations

Station	GLon	GLat	MLon	MLat
Kiana (KIAN)	199.6	67.0	−105.6	65.6
Fort Yukon (FYKN)	214.8	66.6	−92.8	67.7
Gakona (GAKO)	214.9	62.4	−89.9	63.4
White Horse (WHIT)	224.8	61.0	−79.7	63.9
Inuvik (INUV)	226.2	68.4	−83.7	71.6
Fort Simpson (FSIM)	238.8	61.8	−64.9	67.5
Fort Smith (FSMI)	248.1	60.0	−52.3	67.5
Rabbit Lake (RABB)	256.3	58.2	−40.1	67.0
Gillam (GILL)	265.4	56.4	−26.1	66.2
Fort Churchill (FCHU)	265.9	58.8	−25.6	68.5
Rankine Inlet (RANK)	267.9	62.8	−23.1	72.5
Sanikiluaq (SNKQ)	280.8	56.5	−1.9	66.3
Kuujjuaq (KUUJ)	291.6	58.1	14.3	66.7

Note. MLat and MLon are based on the 2010 AACGM model magnetic field and provided by SuperMAG.

development of ionospheric convection from ground magnetic disturbances, which can be generally attributed to the divergence-free part of ionospheric currents. If those currents are Hall currents, which flow in the direction opposite to local ionospheric convection, the longitudinal deflection of a preceding equatorward flow should manifest in changes in the north-south (H) magnetic component.

In addition to the flow braking in the magnetosphere, the ionospheric response may also play a certain role in the deflection of a pre-onset equatorward flow. As the equatorward flow approaches a high-conductance structure, such as pre-existing arc and diffuse auroral band, extending in the east-west direction (as we expect for the pre-onset auroral sequence), FACs are induced by ionospheric polarization at conductance slopes (Ohtani & Yoshikawa, 2016). Such FACs extend in longitude causing ground magnetic disturbances primarily in the east-west direction (i.e., D component), which sensitively depend on the location relative to FACs, and therefore, to the conductance structure. However, in general, the conductance distribution is unknown for individual events, and therefore, it is extremely difficult to identify the cause of observed D disturbances. In contrast, the ionospheric polarization tends to induce electric fields in the direction of conductance gradients in such a way that the total electric field becomes weaker inside the area of enhanced conductance. Accordingly, the deflected convection flow, as well as the Hall current, tends to be oriented along the conductance structure, that is, in the east-west direction, and its direction does not depend on the details of the conductance distribution, even if its intensity does. Therefore, in the present study, we focus on H disturbances, which allows confidently addressing the direction of the zonal convection flow.

The rest of this paper is organized as follows. In Section 2 we examine three auroral substorms with an emphasis on the spatio-temporal structure of auroral electrojets (AEJs) around auroral breakup. In Section 3 we discuss the result focusing on the role of the flow braking in the substorm initiation. In Section 4 we summarize this study.

2. Event Studies

In this section we examine three auroral substorm events, Events 1–3, which reveal different patterns of the pre-onset development of AEJs. We selected Events 1 and 2 because their pre-onset auroral sequences were reported previously, and drew attention as supporting events for the outside-in scenario of substorm initiation. Auroral breakup took place on different sides of the preceding equatorward flow in those events. We selected Event 3 because it makes a good contrast to Events 1 and 2 as its onset was apparently not preceded by an equatorward flow.

In the present study, we use data from white-light all-sky imagers (ASIs) of the ground-based observatory (GBO) component of the Time History of Events and Macroscale Interactions during Substorms (THEMIS) mission (Angelopoulos, 2008; Donovan et al., 2006; Mende et al., 2008). The image time cadence is 3s. We also use ground magnetometer data from THEMIS/GBO (Russell et al., 2008), Canadian Array for Realtime Investigations of Magnetic Activity (CARISMA; Mann et al., 2008), and Geophysical Institute Magnetometer Array (GIMA) stations. The time resolution is 0.5 for the THMIS/GBO magnetometer data, and 1s for the CARISMA and GIMA magnetometer data. Table 1 lists the coordinates of the ground stations that provided either ASI or magnetometer data used in this study. We use the Altitude Adjusted Corrected Geomagnetic (AACGM) coordinates (Shepherd, 2014) throughout this study.

2.1. 25 February 2008 Substorm: Event 1

We start with an auroral breakup that took place on 25 February 2008, which was observed in the field of view (FOV) of the ASI at Gillam (GILL) at premidnight; GILL was at MLT = 22.7 hr at 0530 UT. The subsequent substorm was weak and confined in space as will be shown later. This event was originally reported by Kepko et al. (2009). Figure 2a, which we adopted from Figure 1 of their paper, shows that prior to the initial
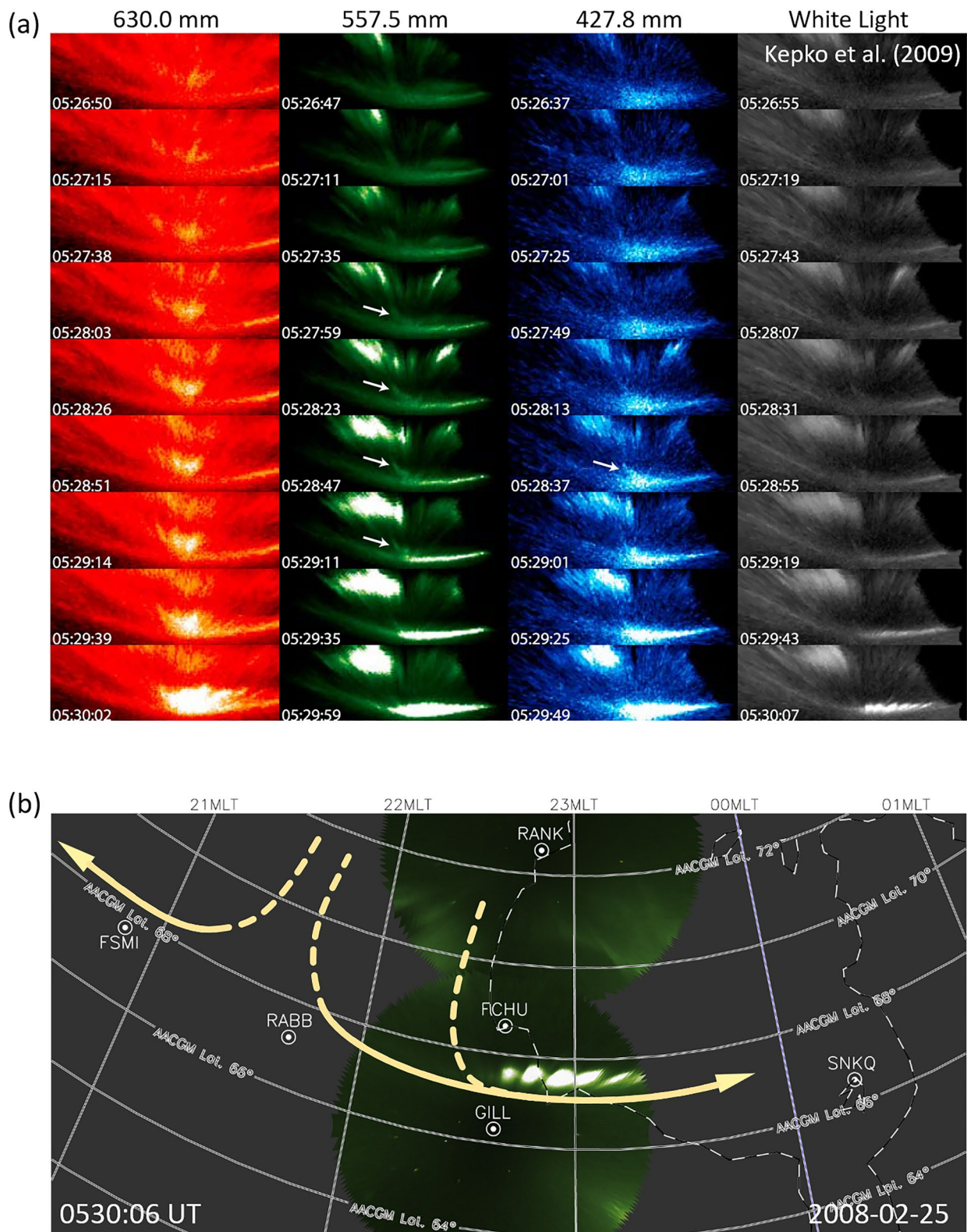
Figure 2. (a) Auroral images in 630.0 mm, 557.7 mm, 427.8 mm, and white light at GILL. Adopted from Figure 1 of Kepko et al. (2009). (b) Auroral mosaic image in white light taken at 0530:06 UT on 25 February 2008. The yellow arrows schematically illustrate pre-onset convection flows inferred from ground magnetic disturbances and the motion of an auroral form.

brightening, a diffuse auroral patch emerged from the background and approached a pre-existing arc from poleward (as identified at the 630.0 nm emission but not at the 557.7 or 427.8 nm emission or in white light). The authors interpreted this diffuse auroral patch as an ionospheric manifestation of an earthward flow burst observed simultaneously in the near-Earth plasma sheet, and concluded that the overall sequence is consistent with the idea that the substorm onset is preceded by the penetration of an earthward flow channel into the near-Earth region (Section 1). Figure 2b shows the auroral mosaic at 0530:06 UT, which basically corresponds to the last row of Figure 2a. See Movie S1 for the entire auroral sequence of this event.

Figure 3 shows magnetic field disturbances observed at GILL and four neighboring stations, Fort Churchill (FCHU), Fort Smith (FSMI), Rabbit Lake (RABB), and Sanikiluaq (SNKQ); see Figure 2b for their locations relative to the breakup auroral arc. H (red) is parallel to the horizontal projection of the average magnetic field and positive northward, and Z (blue) is vertically downward. We focus on these two components in this study because disturbances in the D (eastward) component are often not explainable or essential for addressing the deflection of the equatorward flow (Section 1); see Figure S1 in the Supporting Information S1 for the plot of all three components. Each component of each station is plotted with an arbitrary offset. The three vertical dashed lines mark T0 = 0526:47 UT, when a small arc formed in 427.8 and 577.7 nm at the western edge of the equatorward-moving diffuse red-line patch, T1 = 0529:11 UT, when the initial brightening took place, and T2 = 0530:31 UT, when the poleward expansion started (i.e., auroral breakup). Those timings were adopted from the original study by Kepko et al. (2009; see their Table 1). See also Miyashita and Ieda (2018) for a quantitative timing analysis of the auroral sequence of this event. Figure 2b also shows that auroral beads formed at this substorm onset; auroral beads, longitudinally periodic wavy structures of auroral emission, are a general (>90%) feature of onset arcs observed around initial brightening (e.g., Kalmoni et al., 2017), and in fact, they were also observed in the other two events.

At GILL, H (red) started to decrease at T0, and tended to decrease through the initial brightening (T1) until ∼0531 UT (as hatched in Figure 3), when it started to increase following the auroral breakup at T2. This H increase does not necessarily indicate the decay of the westward AEJ, but it may be attributed to the poleward motion of the westward AEJ. At FCHU, 2.3° poleward of GILL in MLat, H decreased after T1, and Z (blue) increased and then decreased sharply. This H and Z sequence suggests that an enhanced westward AEJ, which was initially located equatorward of FCHU, moved poleward passing over FCHU. At FCHU, H decreased by ∼90 nT after T1 before it reached its negative peak.

At FSMI, 1.7 hr west of GILL in MLT, H started to increase at T0, and continued to increase through T1, when the initial brightening took place at GILL. This is an interesting contrast to the H reduction at GILL, as emphasized by the hatched areas. The associated equivalent currents were directed eastward and westward over FSMI and GILL, respectively. At RABB, which is located between FSMI and GILL in longitude, H changed negatively after T0 in a way similar to the GILL H component; see the purple dashed line below the GILL H component, which shows the RABB H segment multiplied by two and shifted by +37 s in time. H also decreased at SNKQ, 1.6 hr east of GILL in MLT, but it started slightly (∼20 s) after T1.

Assuming that these H variations can be attributed to local ionospheric Hall currents, the corresponding convection can be envisioned as depicted by the yellow arrows in Figure 2b; an equatorward flow proceeding toward somewhere between FSMI and RABB turned eastward and westward as it approached the preexisting arc. The time delay of the H reduction at SNKQ can be attributed to the eastward extension of the eastward-turning flow. We also note that the demarcation meridian between the westward and eastward turning branches was far west of the aforementioned equatorward-moving diffuse auroral form, which was observed near the GILL meridian (Figure 2a). It is possible that the observed auroral form was an internal structure near the eastern edge of a much wider equatorial flow channel; this is conceivable since the MLT separation between RABB and GILL, ∼1 hr, is comparable to the typical MLT width of the ionospheric flow channel (Juusola et al., 2009; Kauristie et al., 2000).

We note that ground magnetic disturbances as we examine in this study represent changes from preceding levels, not from quiet levels, and from those disturbances, we can infer associated transient processes but not background ionospheric currents or convection. More specifically, the convection flows schematically shown in Figure 2b represent a transient meso-scale process, and caution needs to be exercised when addressing them in the context of global convection structures such as the dawn and dusk convection cells and Harang reversal.
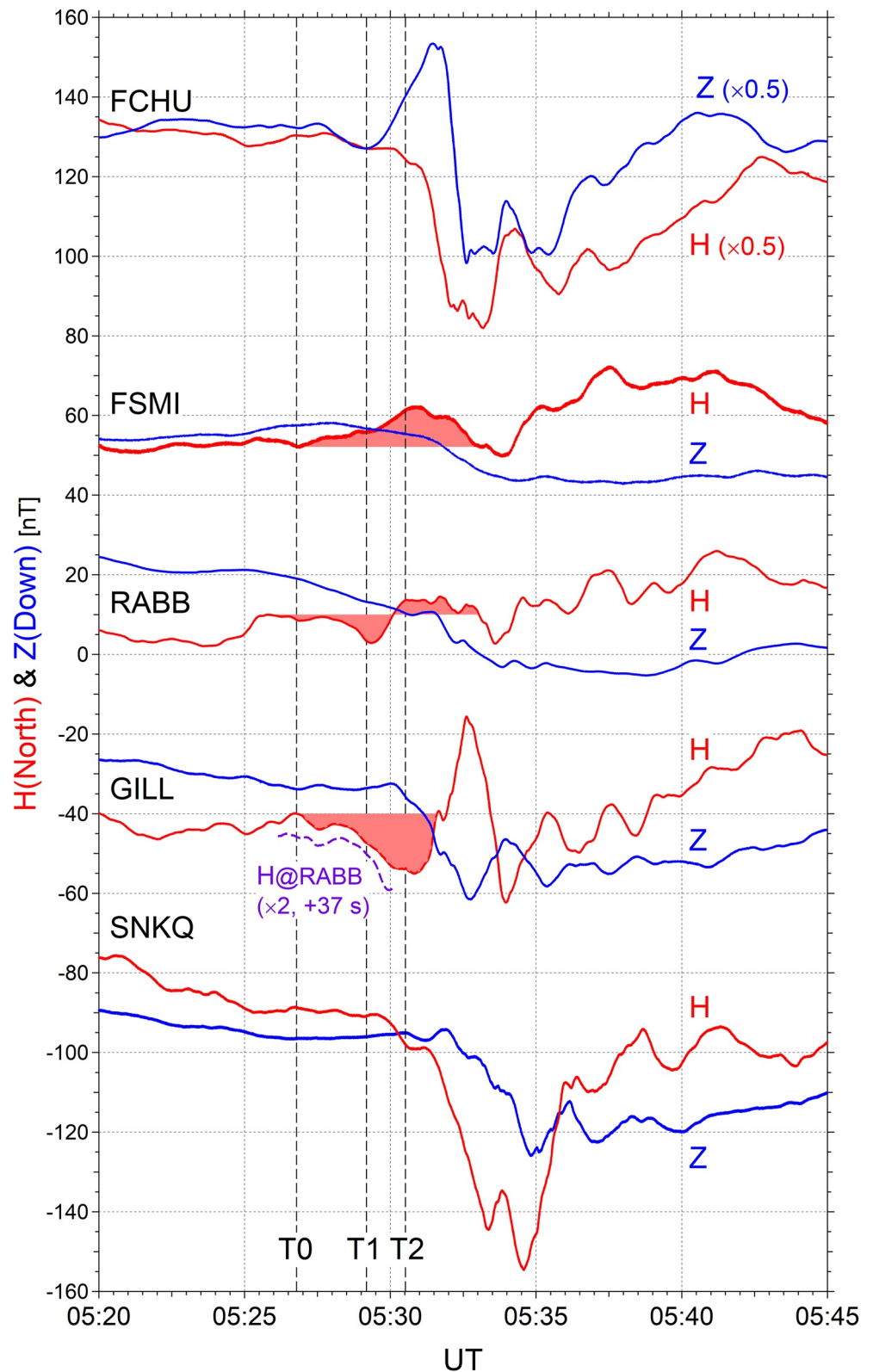
Figure 3. Ground H (red) and Z (blue) magnetic disturbances observed during the interval of 0520–0545 UT on 25 February 2008. The baseline is arbitrary for each plot. T0, T1, and T2 mark 0526:47, 0529:11 (initial brightening), and 0530:31 UT (auroral breakup), respectively.
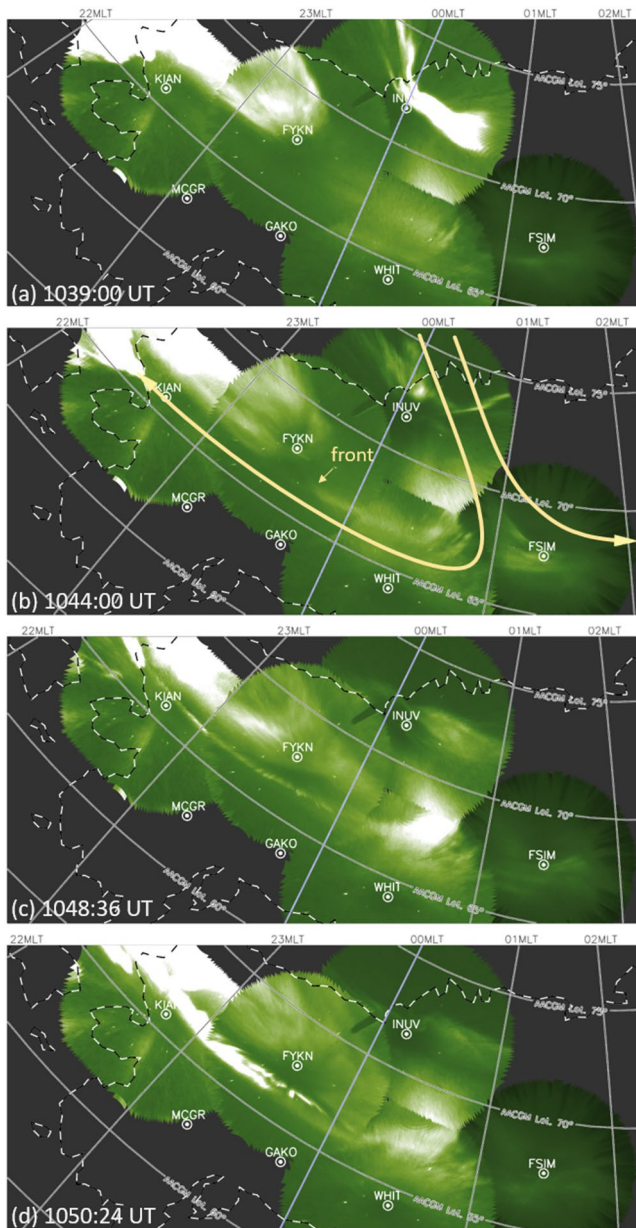
Figure 4. Auroral mosaic images at (a) 1039:00, (b) 1044:00, (c) 1048:36, and (d) 1050:24 UT on 4 February 2008. The yellow arrows in Figure 4b schematically illustrate pre-onset convection flows inferred from ground magnetic disturbances and the motion of an auroral form.

In summary, this auroral substorm event was preceded by an equatorward flow approaching a pre-existing arc, which subsequently turned eastward and westward. The initial brightening and auroral breakup took place at the eastward-turning branch while its front was still proceeding eastward.

2.2. 4 February 2008 Substorm: Event 2

In this subsection we examine an auroral substorm that took place on 4 February 2008, which was observed in the Alaskan sector at premidnight local time. This is one of the three example events that Nishimura et al. (2010a) reported for the initiation of auroral substorms preceded by the approach of an auroral streamer. SML, SuperMAG equivalent to the AL index, was around −200 nT or below for 2 hr before the initial brightening (not shown). Accordingly, aurora was already active on the night side when the event started, and pre-onset ground magnetic disturbances were more complex and larger in magnitude than those observed in Events 1 and 3. As will be shown in the following, the pre-onset auroral streamer made a sharp westward turn in this event as if it followed a convection pattern of the Harang reversal.

Figure 4a shows the auroral mosaic at 1039:00 UT, which shows an auroral streamer crossing the FOV of Inuvik (INUV) from the northwest to the southeast. This auroral streamer reached near the zenith of FSIM and made a sharp westward turn; see Figure 3 of Nishimura et al. (2010a) and Movie S2 for the entire auroral sequence of this event. By 1044 UT the primary turning point had moved westward to the northern part of the FOV of White Horse (WHIT), and the westward intrusion of the auroral intensification halted with its front staying in the southeast of Fort Yukon (FYKN) as shown in Figure 4b. However, at 10:47:30 UT it suddenly started to extend westward crossing the FOV's of FYKN and Kiana (KIAN) in a minute, and then brightened immediately followed by auroral breakup. Figures 4c and 4d show the auroral mosaic images at 1048:36 and 1050:24 UT, slightly after the initial brightening and auroral breakup, respectively.

Figure 5 shows H and Z magnetic disturbances observed at various ground stations for the interval of 1033–1058 UT; see Figure S2 in the Supporting Information S1 for the plot of all three components. The three vertical dashed lines mark 1040:42 UT (T0), when the front of the auroral streamer reached the westward turning point near the zenith of FSIM, 1048:15 UT (T1), when auroral beads started to form following the sudden westward extension of the auroral arc, and 1050:09 UT (T2), when the auroral breakup started.

We start with five lower-latitude stations, from Gakona (GAKO) to GILL from the east to the west. About 2 min before T0, 'w'-shaped H reductions (hatched areas) started at the three eastern stations, Fort Simpson (FSIM), FSMI, and GILL. At each station, the H variations were larger than the Z variations in magnitude, indicating that the source westward current was flowing overhead of the station; as noted earlier, this westward current is not necessarily the AEJ itself, but in general, its disturbance. The phase of the 'w'-shaped variation lagged eastward as guided by the arrows. The phase velocity was roughly 2–3 hr/min in MLT.

At the two western stations, GAKO and WHIT, H changed roughly 180° out of phase from these 'w'-shaped variations. We cannot find any clear phase difference between GAKO and WHIT. At each station the associated Z variations were insignificant suggesting that the source current, an eastward AEJ disturbance, was flowing near the station latitude. The auroral arc located a few degrees north of WHIT (Figure 4b), which possibly corresponded to the poleward border of this eastward AEJ; the eastward AEJ was presumably an ionospheric Hall
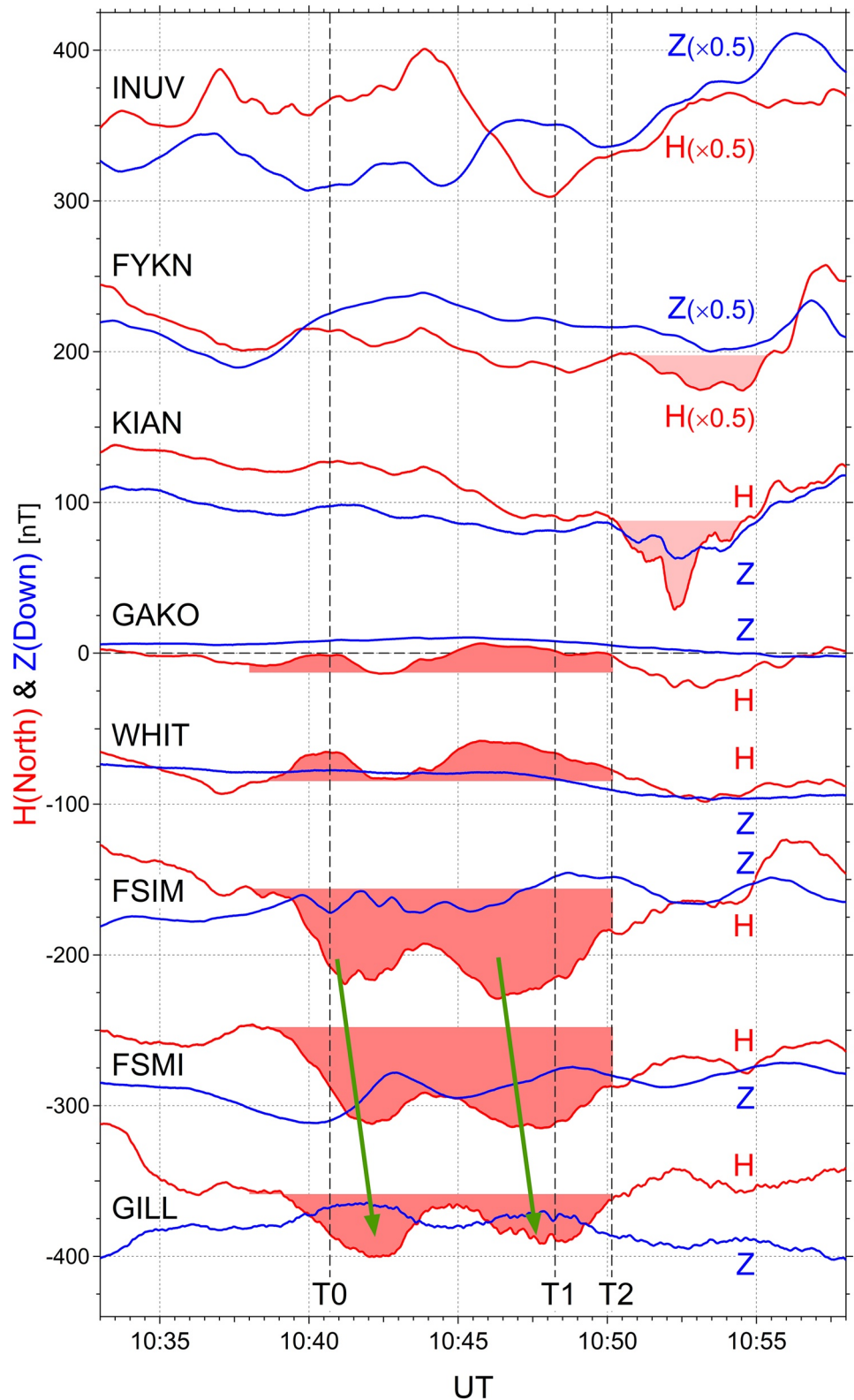
Figure 5. Ground H (red) and Z (blue) magnetic disturbances observed during the interval of 1033–1058 UT on 4 February 2008. The baseline is arbitrary for each plot. T0, T1, and T2 mark 1040:42, 1048:24 (initial brightening), and 1050:15 UT (auroral breakup), respectively. The H and Z variations at INUV and FYKN are factored by 0.5.

current driven by a poleward electric field, and the meridional closure of the associated Pedersen current requires an upward FAC at its poleward edge possibly accompanied by auroral precipitation.

The overall longitudinal structure of these H variations as well as their temporal development is consistent with the idea that the equatorward (more precisely, southeastward) convection flow, as observed as the auroral streamer crossing the INUV FOV, turned eastward and westward at a meridian somewhere between WHIT and FSIM; see the yellow arrows in Figure 4b. The 'w'-shaped and inverted 'w'-shaped H variations suggest that there were two successive intensifications of the equatorward flow. It is, however, difficult to identify two corresponding auroral enhancements as aurora was continuously dynamic (Movie S2). These magnetic variations started prior to T0, which may suggest that the corresponding earthward flow burst in the plasma sheet had a precursor flow (that did not show up in auroral emission), or it may reflect an ionospheric polarization effect as expected for a flow channel approaching a sharp conductance gradient (Ohtani & Yoshikawa, 2016).

At KIAN and FYKN, where the initial brightening took place followed by the auroral breakup, H increased slightly after the initial brightening (T1), but decreased after the auroral breakup (T2) as lightly hatched in Figure 5. The H reduction started slightly earlier and its magnitude was larger at KIAN, which is consistent with the fact that the auroral breakup was centered in the KIAN FOV (Figure 4d). Because of their collocation with the auroral breakup, it should be most reasonable to attribute these H reductions to the westward AEJ segment of a wedge current system although it was apparently short-lived and weak in intensity. Most importantly, no similar H reduction was observed at FSIM as well as FSMI and GILL suggesting that this (onset-related) wedge current system was confined in longitude in the west of the flow demarcation meridian.

Finally we note that the largest H reduction of this event (∼200 nT from peak to peak) was actually observed at INUV before the initial brightening (T1) in association with local auroral activity (Figure 4; Movie S2), which was possibly a poleward boundary intensification (PBI). Therefore, without the ASI images, it would be extremely difficult to identify the timing and location of the onset of this substorm event and understand its development.

In summary, the onset of this auroral substorm was also preceded by the zonal divergence of an equatorward convection flow. Although the eastward-turning branch was more intense, it was at the westward-turning branch that the auroral breakup took place. The post-onset intensification of the westward AEJ, which was presumably the ionospheric segment of a newly formed wedge current system, was apparently confined in the west of the flow demarcation meridian.

2.3. 3 March 2014 Substorm: Event 3

The last event that we examine, Event 3, is different from Events 1 and 2 in the sense that auroral breakup was apparently not preceded by a transient equatorward flow in neighboring sectors. The auroral breakup of this event took place at 0617 UT on 3 March 2014, which was observed at GILL at MLT = 23.5 hr. It was preceded by an hour of steady SMU (100–150 nT; SMU is SuperMAG equivalent to the AU index) and SML (∼−100 nT), and after the auroral breakup SML reached its negative peak <−330 nT at 0622 UT (not shown).

Figure 6 shows auroral mosaic images at selected UT's. At 0612:00 UT, there was an arc extending from FSMI to KUUJ over several hours in MLT across midnight (Figure 6a); this arc turned out to be the onset arc of this event. In the FSMI FOV, this arc was located south of the zenith, around ∼66° in MLat, but barely recognizable until beads formed along it (compare with Figure 6b). The initial brightening took place, along with the beads formation, at 0615:45 UT in the FSIM–FSMI–GILL sector. The arc brightened continuously, and the auroral breakup took place at 0617:00 UT in the GILL FOV (Figures 6b and 6c). Before the breakup there was another thin arc connecting the zeniths of FSMI, RABB, and GILL (Figure 6a), which slowly moved equatorward but did not touch the onset arc before the onset. There was one more arc before the breakup, which stayed around MLat = 69° in the GILL FOV (Figure 6a). Possibly corresponding features can be found in the poleward parts of the FSIM and FSMI FOV's. Most importantly, we could not find any auroral form coming from poleward toward the pre-existing arc before the auroral breakup. See Movie S3 for the entire auroral sequence of this event.

Figure 7 shows ground H and Z magnetic disturbances observed during the interval of 0605–0630 UT; see Figure S3 in the Supporting Information S1 for the plot of all three components. The two vertical dashed lines mark 0615:45 UT (T1), the time of the initial brightening, and 0617:00 UT, the time of the auroral breakup. Magnetometer data from GILL is not available for this event, and we examine data from FCHU instead, which is roughly
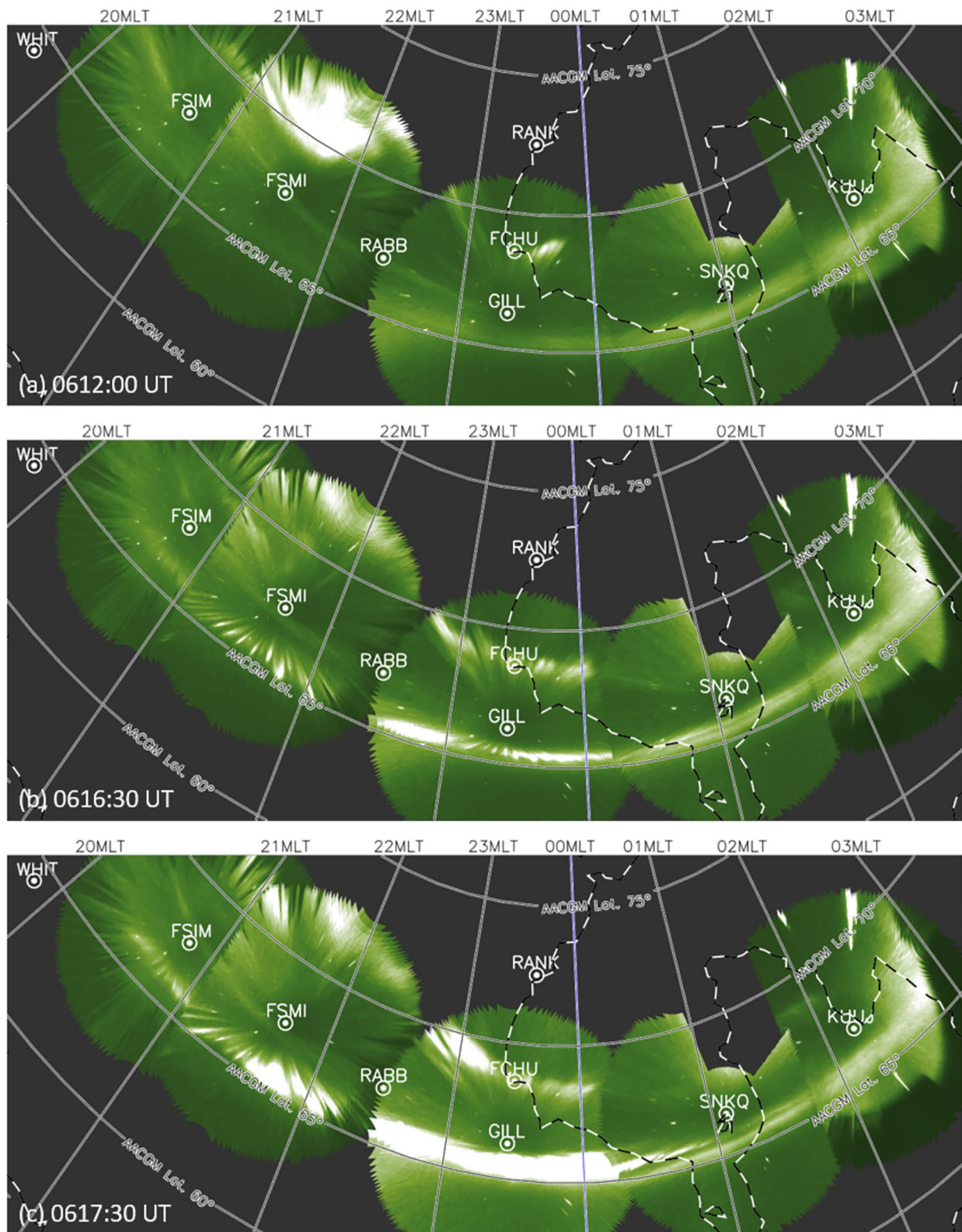
Figure 6. Auroral mosaic images at (a) 0612:00, (b) 0616:30, and (c) 0617:30 UT on 3 March 2014.
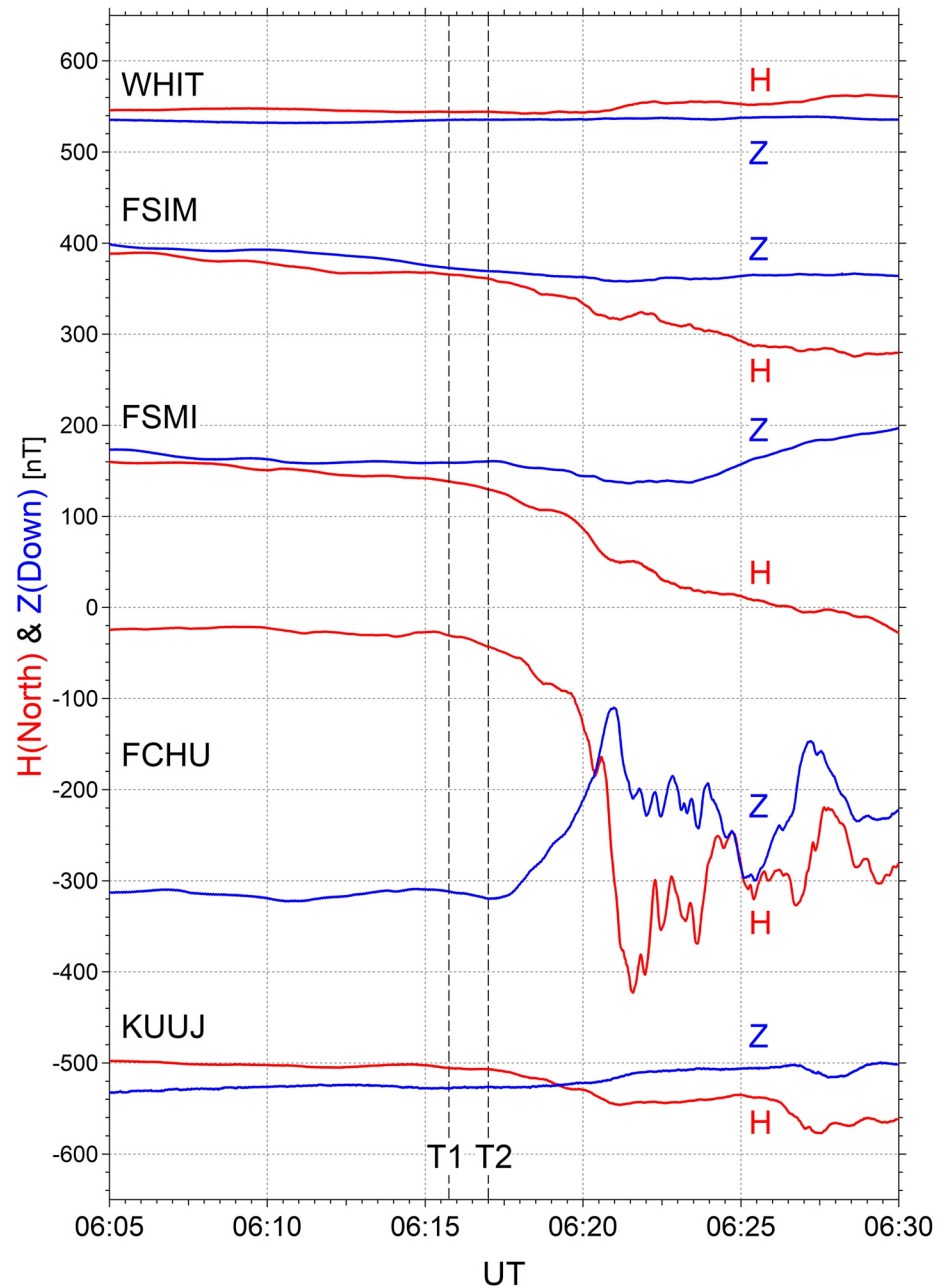
Figure 7. Ground H (red) and Z (blue) magnetic disturbances observed during the interval of 0605–0630 UT on 3 March 2014. The baseline is arbitrary for each plot. T1 and T2 mark 0616:15 (initial brightening) and 0617:15 UT, (auroral breakup), respectively.

at the same meridian as GILL but 2.3° poleward. At FCHU, H started to decrease at, possibly before, T1. The H reduction continued through T2, followed by a sharp reduction starting at 0619:40 UT. H fell to below −300 nT at 0621:30 UT. Z increased after T2, then decreased but stayed positive indicating that the westward AEJ started to intensify equatorward of FCHU and expanded poleward (as suggested by the poleward auroral expansion observed at GILL), but its center stayed equatorward of FCHU.

H also started to decrease gradually around T1 at FSIM and FSMI, and did not change noticeably at WHIT; WHIT, FSIM, and FSMI were 3.6, 2.6 and 1.8 hr west of GILL in MLT, respectively (Figure 6). Farther west of WHIT, no corresponding feature was observed (not shown). Therefore, for this event, we cannot find any combination of positive and negative H disturbances that can be associated with the zonal divergence of an

equatorward flow. This is consistent with the absence of auroral streamers in the corresponding sector. Moreover, H also started to decrease, though slightly, around T1 at KUUJ, 2.7 hr east of GILL. Therefore, the pre-onset H reduction extended at least from FSIM to KUUJ, over 5 hr in MLT, suggesting that the associated enhancement of the westward AEJ was a part of the enhancement of the global two-cell current system (i.e., DP2 system) as we expect for the classical growth phase.

In summary, in contrast to Events 1 and 2, the auroral breakup of this event did not appear to be preceded by the approach of an equatorward flow to the pre-existing arc, but it took place as the westward AEJ enhanced in the entire midnight-to-dawn sector.

3. Discussion

In Section 2 we examined the spatio-temporal development of AEJs around auroral breakup, which we interpreted in the context of ionospheric convection assuming that the observed ground H magnetic disturbances can be attributed to zonal ionospheric Hall currents. As mentioned earlier, those Hall currents reflect transient processes, and in general, they are distinct from global AEJs. Events 1 and 2 were reported previously as examples for the substorm initiation sequence with the preceding approach of equatorward-moving auroral forms (Kepko et al., 2009; Nishimura et al., 2010a). We found that in each event, the preceding equatorward flow turned both eastward and westward. The initial brightening took place at the eastward-turning branch in Event 1 and at the westward-turning branch in Event 2.

As we described in Section 1 (Figure 1), the auroral sequence alone does not tell how the pre-onset equatorward flow behaves as it approaches the equatorward part of the auroral oval, that is, whether (A) the equatorward flow turns sometimes westward but other times eastward, and auroral breakup takes place after the flow turning (Figures 1a and 1b), or (B) the equatorward flow turns both eastward and westward, and auroral breakup takes place sometimes at the westward-turning branch but other times at the eastward-turning branch (Figures 1c and 1d). Apparently (B) was the case for Events 1 and 2.

The difference between (A) and (B) is critically important for understanding the role of the flow braking in substorm initiation. Whereas (A) means no more than that substorm onset is preceded by the penetration and braking of an earthward flow, (B) implies that substorm onset does not have to coincide with the flow braking in time or space. Here we consider that the zonal divergence of the equatorward flow is the ionospheric manifestation of the flow braking; it is difficult to think of any other reason for the earthward flow burst to diverge dawnward and duskward.

For clarification, this zonal flow divergence corresponds to the formation of a pair of clockwise and counter-clockwise convection vortices ($\nabla \times \boldsymbol{v}$), viewed from above the northern ionosphere, on its dusk and dawn sides, respectively, and therefore, the formation of a region-1 (R1) sense wedge current system. This wedge current system is presumably centered at the flow demarcation meridian. However, if the initial brightening takes place after the flow divergence, whether at the eastward- or westward-turning branch, it suggests that in addition to this wedge current system, there is another wedge current system that is directly related to the initial brightening. In other words, even though we usually assume, if implicitly, that the substorm current wedge model applies to the entire sequence of substorm development, we may need to consider that it actually consists of two current systems: one is associated with the pre-onset flow braking, and the other is directly related to the initial brightening and subsequent auroral breakup.

This point is most straightforward for events in which auroral breakup takes place at the eastward turning branch as we found for Event 1. See Figure 8a for a schematic illustration. The onset-related current wedge is considered to extend in longitude as wide as the breakup aurora does, and likely farther eastward as there may be a downward FAC part that is not luminous in auroral emission. Therefore, at onset, this wedge current system extends only east of the flow demarcation meridian. Event 2 provides a different example. In this event the post-onset H reduction, which can be attributed to the ionospheric segment of the onset-related substorm current wedge, was apparently confined in the west of the flow demarcation meridian as schematically shown in Figure 8b. These two events suggest that the two wedge current systems coexist in the early stage of substorm development, and the flow braking is not the direct cause of substorm onset. It is therefore conceivable that some substorms are not
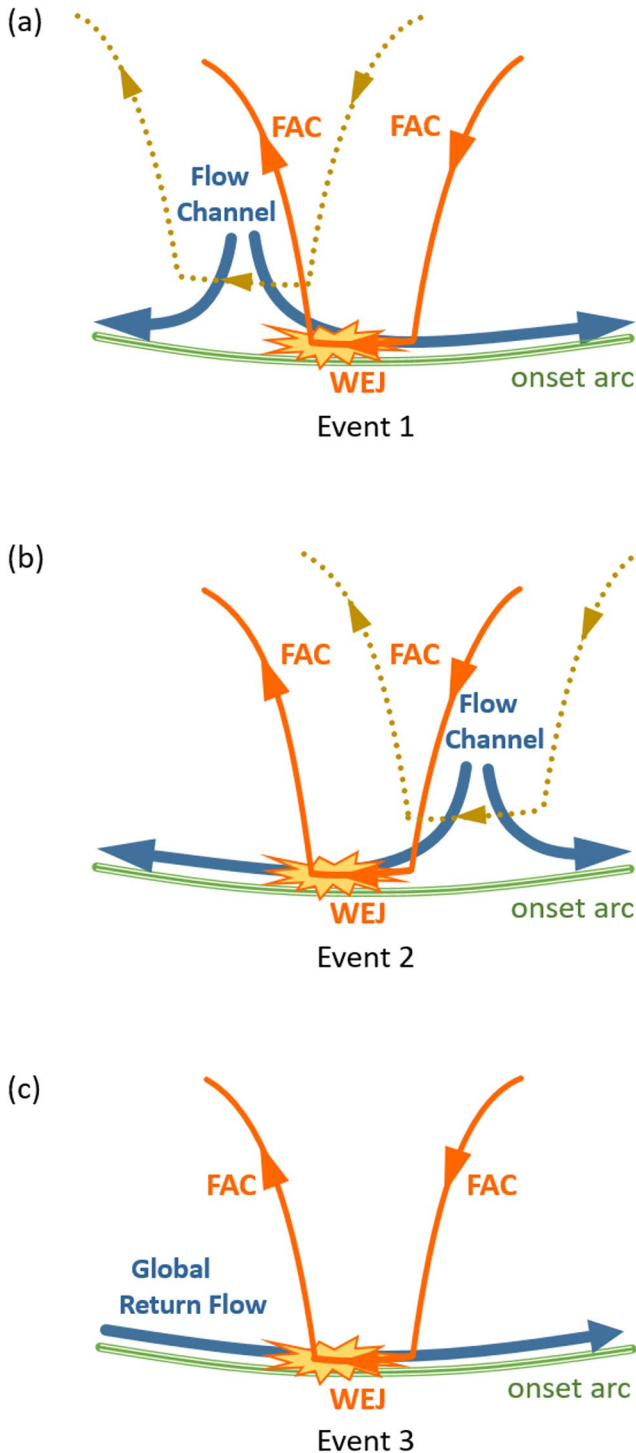
Figure 8. Schematic illustration of the location of auroral breakup relative to the pre-onset equatorward flow channel and wedge current systems expected for the flow braking (dotted yellowish brown) and auroral breakup (orange) for (a) Event 1, (b) Event 2, and (c) Event 3.

preceded by the approach of an equatorward flow as we found for Event 3 (Figure 8c). In such a case the onset-related current wedge is presumably the only element of the substorm current wedge.

The idea that the substorm current wedge consists of two systems may also explain why geosynchronous dipolarization is sustained while the dipolarization region continues to expand earthward as well as azimuthally (Ohtani et al., 2018, 2020), and ground magnetic disturbances are globally coherent even if during the substorm expansion phase, multiple "wedgelets" co-exist corresponding to auroral streamers (Liu et al., 2015; Ohtani & Gjerloev, 2020).

We also note that in reality, the FAC part of the wedge current system is probably not as simple as represented by line currents. For example, the upward FAC collocated with an onset arc apparently pairs with an adjacent downward FAC sheet (Dubyagin et al., 2003; Mende et al., 2003). In such a case, the net FAC, as determined by the local balance between the upward and downward FACs, likely extends along the onset arc, and its polarity (i.e., upward and downward) may change with longitude. Although this additional complexity does not affect the conclusion of the present study (as we inferred the longitudinal extent of wedge current systems from the AEJs), the actual FAC structure is crucial for understanding the substorm initiation process in the magnetosphere.

We examined only three events in this study, and therefore, the generality of the present result needs to be addressed in the future. It is crucial to systematically examine how often pre-onset equatorward flows diverge zonally, and if they do, where auroral breakup takes place relative to the flow demarcation meridian (Figure 1). Nishimura et al. (2010a) reported that in most events substorm onset takes place either near or west of the meridian where the auroral streamer reaches the equatorward part of the auroral oval, and onset rarely takes place east of this contact point (~10%); see their Figure 9c. Since the equatorward convection flow is centered east of the accompanying auroral streamer, the MLT distribution of auroral breakup locations would be skewed farther westward if we refer to equatorward flows rather than auroral streamers. Therefore, according to their result, Event 1, in which auroral breakup took place at the eastward turning branch, belongs to an even smaller (than 10%) minority. For the same reason, in some of majority events (~50%) in which auroral breakup took place near the streamer contact point, auroral breakup may have actually taken place at the westward turning branch.

It is also crucial to examine how often auroral substorms are triggered without a preceding equatorward flow. This issue was addressed by Mende et al. (2011) by examining a subset of the events selected by Nishimura et al. (2010a). Whereas Nishimura et al. (2010a) reported that 84% of 251 auroral intensifications took place following the approach of an auroral form to the onset area, Mende et al. (2011) randomly selected 20 out of those 251 events and reported that the occurrence frequency was 43%. They explained this large difference (84% vs. 43%) in terms of the classification of events with an aurora form approaching from the east/west (without any preceding equatorward motion confirmed), which Nishimura et al. (2010a) counted in their statistics but Mende et al. did not. It should be insightful to examine for such events whether, or where, the AEJ diverges zonally outside of the onset sector (as an indicator of an equatorward flow).

So far we have been addressing the zonal flow divergence as an ionospheric manifestation of the braking of earthward flow bursts in the near-Earth plasma sheet. However, it may be alternatively explained in terms of the equatorward gradient of ionospheric conductance due to auroral precipitation (i.e., ionospheric polarization), which behaves as a wall against an equatorward flow coming from poleward. The process may be envisioned in such a way that equi-contours of electrostatic potential, which form the flow channel away from the conductance gradient, are squeezed out of the higher-conductance area. This explanation is physically the same as the explanation of PBIs proposed by Ohtani and Yoshikawa (2016; see their Figure 5), for which they considered the approach of a polar cap flow to the poleward boundary of the auroral oval.

If the cause of the zonal flow divergence is magnetospheric, the onset arc maps to the transition region, where the magnetic field changes from a stretched to a dipolar configuration, and the flow braking takes place. If the cause of the zonal flow divergence is ionospheric, we still need to understand how it affects the flow braking in the magnetosphere. Nevertheless, the M-I system presumably adjusts itself in such a way that the convection meets local requirements both in the magnetosphere and ionosphere. Or, substorm initiation itself may be a process that makes such an adjustment.

Finally we would like to point out that ground H measurements, if made densely in longitude in the auroral zone, can be used for remotely detecting and characterizing earthward flow channels in the plasma sheet. Although the spacecraft provides the most direct measurement, the satellite detection of earthward flow bursts is severely constrained by the satellite distribution. Auroral imaging has global coverage and is widely used for studying auroral streamers (as an ionospheric manifestation of earthward flow bursts). However, the availability of space-borne global imaging is limited, and ground-based imaging is highly conditional (e.g., local weather, lunar phase, season). The network of ground radars (e.g., SuperDARN) is another alternative, but continuous and global monitoring of such dynamic and meso-scale flows seems to be a challenge as radar echoes are not always measured continuously in time or densely in space. The convergence of zonal ionospheric currents (as identified by H disturbances of opposite signs) could be an indirect measure of equatorward flow channels. Such diverging flows can be observed away from the equatorward flow (i.e., ground stations do not have to be located underneath the flow channel to detect it). The trade-off is that associated ground magnetic disturbances may be difficult to identify if local ionospheric conductance is low or other current systems coexist. Nevertheless, if identified, the zonal flow divergence may serve as a reference time for studying the substorm initiation sequence (Section 2). In addition, with the assistance of modeling efforts, it may be possible to derive the spatial distribution of equatorward flow channels (e.g., Juusola et al., 2009). In particular, the width of the flow channel is essential for quantifying the transport of mass, energy, and magnetic flux. We hope that the present study contributes to better understanding the role of meso-scale processes in storm and substorm dynamics, which is a current focal issue of geospace science.

4. Summary

In the present study we examined three auroral substorms, Events 1–3, and addressed how the AEJ develops in time and space before auroral breakup. In Events 1 and 2, the initial brightening was preceded by the equatorward motion of an auroral form. From the longitudinal distribution of ground H (northward) magnetic disturbances, which we interpreted in terms of the change of local ionospheric Hall currents (i.e., AEJs), we inferred that the associated equatorward flow turned eastward and westward as it approached the equatorward part of the auroral oval. This zonal flow divergence presumably reflected the dawnward and duskward turning of an earthward flow burst in the near-Earth plasma sheet. The initial brightening took place at the eastward-turning branch in Event 1, and at the westward-turning branch in Events 2. The center of the onset-related current wedge was apparently displaced eastward and westward from the zonal flow demarcation meridian in Events 1 and 2, respectively. For Event 3, we could not find any auroral or AEJ signature indicative of the pre-onset approach of an equatorward flow. These results suggest that even though the auroral sequence of substorm initiation is often addressed in terms of the braking of an earthward flow burst, (a) the flow braking is not necessarily the direct cause of substorm onset, and (b) the substorm wedge current system consists of two elements, one that results from the flow braking and the other that formed at substorm onset and develops subsequently, and the former is absent for substorms that are not preceded by the flow braking.

Data Availability Statement

THEMIS/GBO ASI and GMAG data, CARISMA data, and GIMA data are available at http://themis.ssl.berkeley.edu/data_files.shtml. CARISMA magnetometer data are also available at https://www.carisma.ca/carisma-data-repository.

References

Akasofu, S.-I. (1964). The development of the auroral substorm. *Planetary and Space Science*, *12*, 273–282. https://doi.org/10.1016/0032-0633(64)90151-5

Angelopoulos, V. (2008). The THEMIS mission. *Space Science Reviews*, *141*(1–4), 5–34. https://doi.org/10.1007/s11214-008-9336-1

Birn, J., Hesse, M., Haerendel, G., Baumjohann, W., & Shiokawa, K. (1999). Flow braking and the substorm current wedge. *Journal of Geophysical Research*, *104*(A9), 19895–19903. https://doi.org/10.1029/1999JA900173

Donovan, E., Mende, S., Jackel, B., Frey, H., Syrjäsuo, M., Voronkov, I., et al. (2006). The THEMIS all-sky imaging array-system design and initial results from the prototype imager. *Journal of Atmospheric and Solar-Terrestrial Physics*, *68*, 1472–1487. https://doi.org/10.1016/j.jastp.2005.03.027

Dubyagin, S. V., Sergeev, V. A., Carlson, C. W., Marple, S. R., Pulkkinen, T. I., & Yahnin, A. G. (2003). Evidence of near-Earth breakup location. *Geophysical Research Letters*, *30*, 1282. https://doi.org/10.1029/2002GL016569

Frey, H. U. (2010). Comment on "substorm triggering by new plasma intrusion: THEMIS all-sky imager observations" by Y. Nishimura et al. *Journal of Geophysical Research*, *115*, A12232. https://doi.org/10.1029/2010JA016113

Frey, H. U., Mende, S. B., Angelopoulos, V., & Donovan, E. F. (2004). Substorm onset observations by IMAGE-FUV. *Journal of Geophysical Research*, *109*, A10304. https://doi.org/10.1029/2004JA010607

Friedrich, E., Samson, J. C., Voronkov, I., & Rostoker, G. (2001). Dynamics of the substorm expansive phase. *Journal of Geophysical Research*, *106*(A7), 13145–13163. https://doi.org/10.1029/2000JA000292

Gjerloev, J. W., Hoffman, R. A., Sigwarth, J. B., & Frank, L. A. (2007). Statistical description of the bulge-type auroral substorm in the far ultraviolet. *Journal of Geophysical Research*, *112*, A07213. https://doi.org/10.1029/2006JA012189

Henderson, M. G., Reeves, G. D., & Murphree, J. S. (1998). Are north-south aligned auroral structures an ionospheric manifestation of bursty bulk flows? *Geophysical Research Letters*, *25*(19), 3737–3740. https://doi.org/10.1029/98GL02692

Juusola, L., Nakamura, R., Amm, O., & Kauristie, K. (2009). Conjugate ionospheric equivalent currents during bursty bulk flows. *Journal of Geophysical Research*, *114*, A04313. https://doi.org/10.1029/2008JA013908

Kalmoni, N. M. E., Rae, I. J., Murphy, K. R., Forsyth, C., Watt, C. E. J., & Owen, C. J. (2017). Statistical azimuthal structuring of the substorm onset arc: Implications for the onset mechanism. *Geophysical Research Letters*, *44*, 2078–2087. https://doi.org/10.1002/2016GL071826

Kauristie, K., Sergeev, V. A., Kubyshkina, M., Pulkkinen, T. I., Angelopoulos, V., Phan, T., et al. (2000). Ionospheric current signatures of transient plasma sheet flows. *Journal of Geophysical Research*, *105*(A5), 10677–10690. https://doi.org/10.1029/1999JA900487

Kepko, L., McPherron, R. L., Amm, O., Apatenkov, S., Baumjohann, W., Birn, J., et al. (2015). Substorm current wedge revisited. *Space Science Reviews*, *190*, 1–46. https://doi.org/10.1007/s11214-014-0124-9

Kepko, L., Spanswick, E., Angelopoulos, V., Donovan, E., McFadden, J., Glassmeier, K.-H., et al. (2009). Equatorward moving auroral signatures of a flow burst observed prior to auroral onset. *Geophysical Research Letters*, *36*, L24104. https://doi.org/10.1029/2009GL041476

Liou, K., Newell, P. T., Sibeck, D. G., Meng, C.-I., Brittnacher, M., & Parks, G. (2001). Observation of IMF and seasonal effects in the location of auroral substorm onset. *Journal of Geophysical Research*, *106*(A4), 5799–5810. https://doi.org/10.1029/2000JA003001

Liu, J., Angelopoulos, V., Chu, X., Zhou, X.-Z., & Yue, C. (2015). Substorm current wedge composition by wedgelets. *Geophysical Research Letters*, *42*, 1669–1676. https://doi.org/10.1002/2015GL063289

Lui, A. T. Y. (1996). Current disruption in the Earth's magnetosphere: Observations and models. *Journal of Geophysical Research*, *101*(A6), 13067–13088. https://doi.org/10.1029/96JA00079

Lyons, L. R., Nishimura, Y., Shi, Y., Zou, S., Kim, H.-J., Angelopoulos, V., et al. (2010). Substorm triggering by new plasma intrusion: Incoherent-scatter radar observations. *Journal of Geophysical Research*, *115*, A07223. https://doi.org/10.1029/2009JA015168

Machida, S., Miyashita, Y., Ieda, A., Nishida, A., Mukai, T., Saito, Y., & Kokubun, S. (1999). GEOTAIL observations of flow velocity and north-south magnetic field variations in the near and mid-distant tail associated with substorm onsets. *Geophysical Research Letters*, *26*, 635–638. https://doi.org/10.1029/1999gl900030

Mann, I. R., Milling, D. K., Rae, I. J., Ozeke, L. G., Kale, A., Kale, Z. C., et al. (2008). The upgraded CARISMA magnetometer array in the THEMIS era. *Space Science Reviews*, *141*, 413–451. https://doi.org/10.1007/s11214-008-9457-6

McPherron, R. L., Russell, C. T., & Aubry, M. P. (1973). Satellite studies of magnetospheric substorms on August 15, 1968: 9. Phenomenological model for substorms. *Journal of Geophysical Research*, *78*, 3131–3149. https://doi.org/10.1029/JA078i016p03131

Mende, S. B., Carlson, C. W., Frey, H. U., Peticolas, L. M., & Østgaard, N. (2003). FAST and IMAGE-FUV observations of a substorm onset. *Journal of Geophysical Research*, *108*(A9), 1344. https://doi.org/10.1029/2002JA009787

Mende, S. B., Frey, H. U., Angelopoulos, V., & Nishimura, Y. (2011). Substorm triggering by poleward boundary intensification and related equatorward propagation. *Journal of Geophysical Research*, *116*, A00I31. https://doi.org/10.1029/2010JA015733

Mende, S. B., Harris, S. E., Frey, H. U., Angelopoulos, V., Russell, C. T., Donovan, E., et al. (2008). The THEMIS array of ground-based observatories for the study of auroral substorms. *Space Science Reviews*, *141*(1–4), 357–387. https://doi.org/10.1007/s11214-008-9380-x

Miyashita, Y., & Ieda, A. (2018). Revisiting substorm events with preonset aurora. *Annals of Geophysics*, *36*, 1419–1438. https://doi.org/10.5194/angeo-36-1419-2018

Murphy, K. R., Mann, I. R., Rae, I. J., Walsh, A. P., & Frey, H. U. (2014). Inner magnetospheric onset preceding reconnection and tail dynamics during substorms: Can substorms initiate in two different regions? *Journal of Geophysical Research: Space Physics*, *119*, 9684–9701. https://doi.org/10.1002/2014JA019795

Nagai, T., Fujimoto, M., Saito, Y., Machida, S., Terasawa, T., Nakamura, R., et al. (1998). Structure and dynamics of magnetic reconnection for substorm onsets with Geotail observations. *Journal of Geophysical Research*, *103*(A3), 4419–4440. https://doi.org/10.1029/97JA02190

Nakamura, R., Baumjohann, W., Schödel, R., Brittnacher, M., Sergeev, V. A., Kubyshkina, M., et al. (2001). Earthward flow bursts, auroral streamers, and small expansions. *Journal of Geophysical Research*, *106*(A6), 10791–10802. https://doi.org/10.1029/2000JA000306

Nishimura, Y., Lyons, L., Zou, S., Angelopoulos, V., & Mende, S. (2010a). Substorm triggering by new plasma intrusion: THEMIS all-sky imager observations. *Journal of Geophysical Research*, *115*, A07222. https://doi.org/10.1029/2009ja015166

Nishimura, Y., Lyons, L. R., Zou, S., Angelopoulos, V., & Mende, S. B. (2010b). Reply to comment by Harald U. Frey on "substorm triggering by new plasma intrusion: THEMIS all-sky imager observations. *Journal of Geophysical Research*, *115*, A12233. https://doi.org/10.1029/2010JA016182

Ohtani, S., Creutzberg, F., Mukai, T., Singer, H., Lui, A. T. Y., Nakamura, M., et al. (1999). Substorm onset timing: The December 31, 1995, event. *Journal of Geophysical Research*, *104*(A10), 22713–22727. https://doi.org/10.1029/1999JA900209

Ohtani, S., & Gjerloev, J. W. (2020). Is the substorm current wedge an Ensemble of wedgelets? Revisit to midlatitude positive bays. *Journal of Geophysical Research: Space Physics*. https://doi.org/10.1029/2020JA027902

Ohtani, S., Motoba, T., Gkioulidou, M., Takahashi, K., & Singer, H. J. (2018). Spatial development of the dipolarization region in the inner magnetosphere. *Journal of Geophysical Research: Space Physics*, *123*, 5452–5463. https://doi.org/10.1029/2018ja025443

Ohtani, S., Motoba, T., Takahashi, K., & Califf, S. (2020). Generalized substorm current wedge model: Two Types of dipolarizations in the inner magnetosphere. *Journal of Geophysical Research: Space Physics*, *125*. https://doi.org/10.1029/2020JA027890

Ohtani, S., & Yoshikawa, A. (2016). The initiation of the poleward boundary intensification of auroral emission by fast polar cap flows: A new interpretation based on ionospheric polarization. *Journal of Geophysical Research: Space Physics*, *121*, 10910–10928. https://doi.org/10.1002/2016JA023143

Russell, C. T., Chi, P. J., Dearborn, D. J., Ge, Y. S., Kuo-Tiong, B., Means, J. D., et al. (2008). THEMIS ground-based magnetometers. *Space Science Reviews*, *141*(1–4), 389–412. https://doi.org/10.1007/s11214-008-9337-0

Samson, J. C., Lyons, L. R., Newell, P. T., Creutzberg, F., & Xu, B. (1992). Proton aurora and substorm intensifications. *Geophysical Research Letters*, *19*(21), 2167–2170. https://doi.org/10.1029/92gl02184

Sergeev, V. A., Liou, K., Meng, C.-I., Newell, P. T., Brittnacher, M., Parks, G., & Reeves, G. D. (1999). Development of auroral streamers in association with localized impulsive injections to the inner magnetotail. *Geophysical Research Letters*, *26*(3), 417–420. https://doi.org/10.1029/1998GL900311

Shepherd, S. G. (2014). Altitude-adjusted corrected geomagnetic coordinates: Definition and functional approximations. *Journal of Geophysical Research: Space Physics*, *119*, 7501–7521. https://doi.org/10.1002/2014JA020264

Shiokawa, K., Baumjohann, W., & Haerendel, G. (1997). Braking of high-speed flows in the near-Earth tail. *Geophysical Research Letters*, *10*, 1179–1182. https://doi.org/10.1029/97gl01062

Wolf, R. A., Wan, Y., Xing, X., Zhang, J.-C., & Sazykin, S. (2009). Entropy and plasma sheet transport. *Journal of Geophysical Research*, *114*, A00D05. https://doi.org/10.1029/2009JA014044

Yang, J., Toffoletto, F. R., Wolf, R. A., Sazykin, S., Ontiveros, P. A., & Weygand, J. M. (2012). Large-scale current systems and ground magnetic disturbance during deep substorm injections. *Journal of Geophysical Research*, *117*, A04223. https://doi.org/10.1029/2011JA017415

Zesta, E., Lyons, L., & Donovan, E. (2000). The auroral signature of Earthward flow bursts observed in the magnetotail. *Geophysical Research Letters*, *27*(20), 3241–3244. https://doi.org/10.1029/2000gl000027